Ernst Schering Foundation Symposium Proceedings, Vol. 5, pp. 245–263
DOI 10.1007/2789_2007_054

Published Online: 25 July 2007

Tumorigenic Epithelial Stem Cells and Their Normal Counterparts

V.S. Donnenberg, J.D. Luketich, R.J. Landreneau, J.A. DeLoia, P. Basse, A.D. Donnenberg(✉)

Hillman Cancer Research Pavilion, 5117 Centre Avenue, Suite 2.42, 15213 Pittsburgh, USA
email: *donnenbergad@upmc.edu*

Abstract. ABC transporters are highly conserved and represent a major protective mechanism for barrier tissues as well as adult tissue stem cells. Emerging data support the existence of a cancer stem cell that shares features of tissue stem cells, including the ability to self-renew and undergo dysregulated differentiation. Here we show that a rare population of cells coexpressing MDR transporters and stem cell markers is a common feature across therapy-naive epithelial cancers as well as normal epithelial tissue. MDR^+ and MDR^- candidate

tumor stem and progenitor populations were all capable of generating highly anaplastic transplantable human tumors in NOD/SCID. The finding that rare cells bearing stem cell markers and having intrinsic MDR expression and activity are already present within the tumorigenic compartment before treatment with cytotoxic agents is of critical importance to cancer therapy. Just as damaged normal epithelial tissues regenerate after chemotherapy by virtue of highly protected resting tissue stem cells, the existence of malignant counterparts in therapy-naive epithelial cancers suggests a common mechanism by which normal and tumor stem cells protect themselves against toxic injury.

1 Background

Multiple drug resistance (MDR) was early recognized as a barrier to cancer therapy (Biedler et al. 1970). The common mechanism responsible for cross-resistance to multiple structurally unrelated agents was determined to be reduced cellular permeability (Ling and Thompson 1974), mediated by a family of highly conserved proteins known as ATP-binding cassette (ABC) transporters (Leslie et al. 2005). Although ABC transporter expression is recognized as a significant cause of chemotherapy resistance, the prevalent paradigm understands MDR in cancer to result from drug-mediated selection of cells with ABC transporter gene amplification (Chen et al. 2002) or regional gene activation (Wang et al. 2006). More recently, it has become apparent that normal adult tissue stem cells, including hematopoietic (Udomsakdi et al. 1991; Chaudhary and Roninson 1991; Goodell et al. 1996), airway (Giangreco et al. 2004), pituitary (Chen et al. 2005), small intestine (He et al. 2005), and testes (Riou et al. 2005), express high levels of MDR transporter activity. Persistence of tissue stem cells is essential to tissue maintenance and repair, and constitutive MDR activity is thought to be one of several mechanisms by which normal tissue stem cells protect themselves from toxic insults, including those resulting from damage by chemotherapeutic agents (Donnenberg and Donnenberg 2005). A dramatic example can be found in chemotherapy-induced alopecia, which results from damage to the rapidly cycling progenitor cells of the hair follicle (Paus and Cotsarelis 1999; Alonso and Fuchs 2003). However, alopecia is reversed on cessation of therapy because the common precursor of the four distinct cell types within the follicle, as well as skin epithelial cells

themselves, is a resting epithelial stem cell (Rendl et al. 2005), which is protected by constitutive MDR activity (Yano et al. 2005).

The cancer stem cell paradigm (Fiala 1968; Hamburger and Salmon 1977; Reya et al. 2001; Dick 2003; Al-Hajj et al. 2004; Donnenberg and Donnenberg 2005; Dick and Lapidot 2005; Wicha et al. 2006; Polyak and Hahn 2006) envisions the cancer-initiating cell as a genetically damaged tissue stem cell, or a more mature cell that has reacquired stem cell attributes through mutation. The unique insight that we derive from the study of adult tissue stem cells is that drug resistance is a normal self-protective mechanism that may be retained by the nascent neoplasm on transformation of the tissue stem cell. The notion that the cancer stem cell, or a subset of these cells, may have constitutive drug resistance agrees with the observation that cancers often recur after apparently successful therapy.

2 Results

2.1 ABGG2$^+$ Cells Are Present in Therapy-Naive Tumor and Normal Lung and Express Stem/Progenitor Markers

Stem cells from a variety of epithelial tissues have been enriched by sorting for cells with constitutive MDR transporter activity. To investigate expression of the MDR transporter ABCG2 in freshly isolated therapy-naive epithelial tumor cells, single-cell suspensions were prepared from solid tumors, malignant ascites, and effusions. Normal lung tissue was also investigated as a positive control. A population of non-hematopoietic, cytokeratin$^+$, ABCG2$^+$ cells was present at low frequency in both neoplastic and normal tissues (Fig. 1).

All newly diagnosed untreated epithelial tumors contained a rare subset of CD45$^-$ cytokeratin^{dim} ABCG2$^+$ cells (0.43±0.57% of CD45$^-$ cells, mean±SD). ABCG2$^+$ cytokeratin^{dim} cells also expressed CD44 (69±18%) and the stem/progenitor markers CD90 (62±20%), CD117 (34±23%), and CD133 (25±23%). Eight ± five percent of ABCG2$^+$ cells (0.03% of CD45$^-$ cytokeratin^{dim}) had low forward and side light scatter profiles compatible with small resting morphology.

None of these markers, alone or in combination, was able to distinguish normal lung from primary epithelial tumors. In contrast, ABCG2$^+$ cells from previously untreated metastatic cancers (effusions and as-

Fig. 1. Expression of ABCG2 and stem cell markers on freshly isolated normal lung tissue and therapy-naive malignant cells. To investigate expression of the MDR transporter ABCG2 in freshly isolated therapy-naive tumor cells, single-cell suspensions were prepared from solid tumors (lung cancer 7, ovarian cancer 3) and malignant ascites and effusions (lung cancer 2, ovarian cancer 6, gastric cancer 1) by mechanical dissection and collagenase digestion. Samples were stained by seven-color flow cytometry for expression of ABCG2, CD45, intracellular cytokeratin, CD44, CD90, CD117, and CD133. An average of 2.5 million events were acquired for each sample (min=200,000, max=6,000,000). The *first row* shows the gating strategy used in this and subsequent analyses. Forward scatter pulse height (*x-axis*) and pulse width (*y-axis*) are used to define singlet cells and eliminate cell clusters. Forward and side light scatter are then used to eliminate debris and dead cells. CD45 expression and side light scatter are used to eliminate hematopoietic cells. The *second row* shows ABCG2 and cytokeratin expression in the gated population of representative normal lung, lung tumor, metastatic lung pleural effusion, and ovarian ascites. The percentages of $ABCG2^+$ $cytokeratin^+$ cells are shown. The average frequency of these cells at each site is shown in the *first bar graph* (*error bars*=SEM). The *remaining bar graphs* show the frequencies of cells with resting morphology (lymphoid light scatter), CD44, CD90, CD117, and CD133 expression in the $CD45^-$, $ABCG2^+$, $cytokeratin^+$ population

cites) had significantly lower proportions of $CD90^+$ and $CD117^+$ cells ($p = 0.034$, and 0.011, respectively) and a higher proportion of $CD133^+$ cells ($p = 0.015$) than either normal lung or primary tumor. These data demonstrate that therapy-naive epithelial tumors contain a rare subpopulation of MDR-positive, stem cell marker-positive cells, a phenotype shared with an equally rare subset present in normal lung tissue. Further, this subpopulation was detectable in malignant effusions and ascites, sites unlikely to harbor normal tissue stem cells. Together these data suggest that stem cells within the tumor are not simply normal stem cells engaged in wound healing, and that these tumor cells share mechanisms with normal tissue stem cells that may equally confer resistance to cytotoxic therapy.

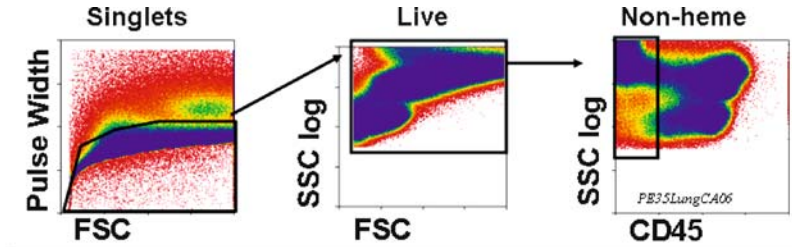
Singlets
Live
Non-heme
Pulse Width
FSC
SSC log
FSC
SSC log
CD45
PE35LungCA06

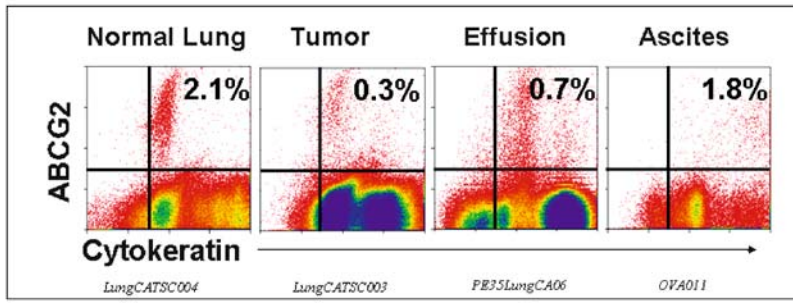
Normal Lung
Tumor
Effusion
Ascites
2.1%
0.3%
0.7%
1.8%
ABCG2
Cytokeratin
LungCATSC004
LungCATSC003
PE35LungCA06
OVA011

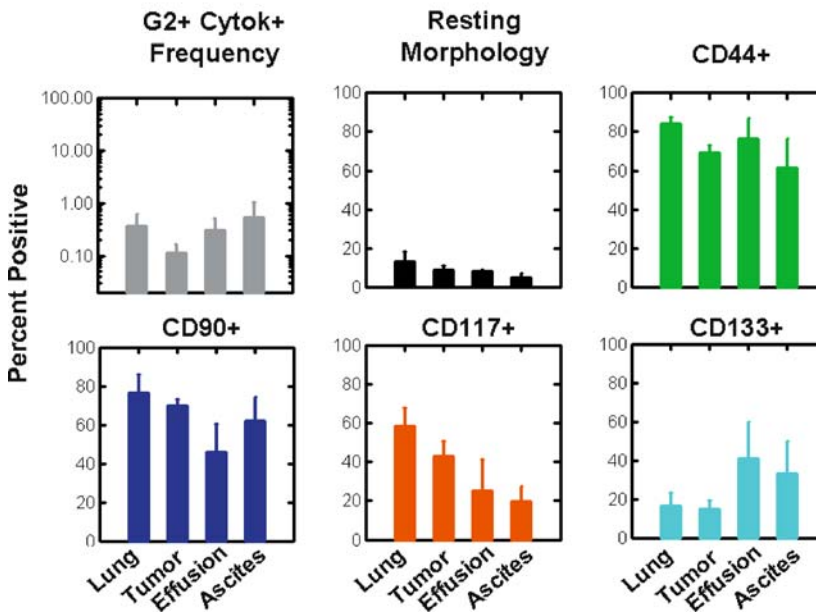
G2+ Cytok+ Frequency
Resting Morphology
CD44+
CD90+
CD117+
CD133+
Percent Positive
100.00
10.00
1.00
0.10
100
80
60
40
20
0
Lung
Tumor
Effusion
Ascites

2.2 ABC Transporters Are Constitutively Active in a Small Subset of Therapy-Naive Tumor Cells

Functional measurement of ABC transporter activity is important, since expression and activity are not always well correlated (Webb et al. 1996). In Fig. 2 we show simultaneous transport of the MDR transporter substrates Hoechst 33342 and R123 in freshly isolated cells from a therapy-naive non-small cell lung tumor. The SP phenotype (ABCG2- and ABCB1-mediated transport) comprised 4% of nonhematopoietic cells, 29% of which had concomitant R123 efflux (ABCB1 transport; Fig. 2, color-evented red). None of the SP negative cells (Hoechst bright) transported rhodamine.

Virtually all of the *dual transporting* cells exhibited low light scatter, consistent with a resting morphology. The ABC transporter specificity of dye efflux was demonstrated with the ABCG2-specific inhibitor fumitremorgin, which abrogated 75% of the SP phenotype. $CD90^+$ cells were present in both SP^+ and SP^- fractions, indicating that not all cells bearing this stem cell marker have MDR activity. Furthermore, when we examined R123 efflux among the $CD45^-$ $CD117^+$ subset of untreated ovarian and lung tumor cells, MDR activity was restricted to the subset with low morphologic complexity and G_1/G_0 cell cycle phase ($n = 5$, data not shown). All epithelial tumors contained a small subpopulation of stem marker$^+$ cells having resting morphology. Figure 3 shows imaging flow cytometry performed on an untreated freshly isolated non small cell lung tumor. The $CD45^-$ $CD90^+$ stem fraction shown in panel A comprised 5% of $CD45^-$ singelt cells and were of uniform small morphology with high nucleus to cytoplasm ratio. In contrast, $CD90^-$ cells comprised the vast majority of $CD45^-$ tumor cells and were heterogenous with respect to morphology. Taken together, these data demonstrate that resting stem cell marker-positive tumor cells with low morphologic complexity express both ABCG2 (breast cancer resistance protein 1) and ABCB1 (P-glycoprotein) and exhibit the highest constitutive MDR activity.

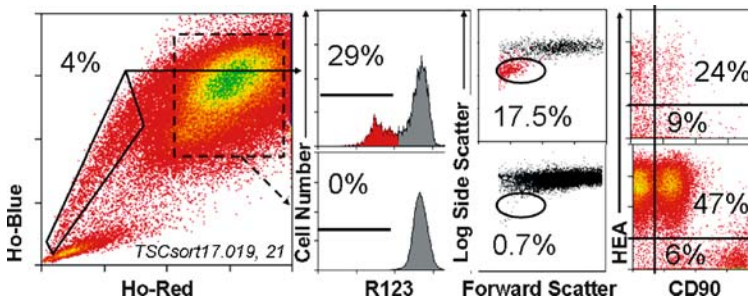

Fig. 2. ABCG2 and ABCB1 activity in freshly isolated therapy-naive non-small cell lung cancer. Antibody-stained suspended tumor cells were incubated simultaneously with the ABCG2/ABCB1 substrate Hoechst 33342 (8 μM) plus the ABCB1 substrate rhodamine 123 (R123, 0.13 μM) for 90 min at 37°C (Bertoncello and Williams 2004). Hoechst emission was separated with a 510-nm dichroic long-pass filter. Blue and red fluorescence were measured with 450-65 nm and 670-20 nm bandpass filters, respectively. Propidium iodide (PI, 10 μg/mL) was added immediately before sample acquisition. All events were gated on PI-excluding (live), nonhematopoietic singlets. Five million events were collected. The *leftmost panel* shows a small population (4%) of Hoechst 33342-excluding cells in the typical pattern of the side population (SP). SP (*top panels*) and non-SP cells (*bottom panels*) were further characterized: A proportion of SP cells also excluded the ABCB1 substrate dye R123. These accounted for 29% of the SP cells (color-evented red in the dot plots) and accounted for almost all of the cells with low forward and side light scatter, consistent with a resting morphology (Fig. 3). Non-SP cells did not transport R123 and were exclusively of high light scatter. A significant proportion of both SP and non-SP cells expressed CD90, often in combination with epithelium-specific antigen HEA. Coincubation of tumor cells with Hoechst 33342, R123, and the ABCG2-specific inhibitor fumitremorgin (10 μM) resulted in 75% inhibition of the SP phenotype

2.3 Transporter-Positive and -Negative Cells Are Tumorigenic

In order to determine tumorigenicity of ABCG2 protected fractions, particularly the resting fraction, ABCG2-positive and -negative $CD90^+$ cell populations were sorted from a recurrent breast cancer pleural effusion. These populations were defined within the $CD45^-$ $CD44^+$ frac-

Fig. 3. A,**B** $CD45^-$ $CD90^+$ cells isolated from primary tumors have small resting morphology. A freshly resected untreated non-small cell lung cancer was collagenase digested and stained with CD45, CD90, and the nuclear stain Draq5 (5 μM). Virtual sorting was performed with an Amnis ImageStream100 imaging flow cytometer (Amnis Corporation, Seattle WA). All analyzed cells were singlets, as determined by a histogram of brightfield area versus brightfield aspect ratio. Images are composites of brightfield, CD90 (*false-colored green*), and Draq5 (*false-colored red*). **A** Images of nonhematopoietic ($CD45^-$) $CD90^+$ cells. **B** Images from consecutive $CD45^-$ $CD90^-$ cells. $CD90^+$ tumor cells were small, with a relatively high nucleus-to-cytoplasm ratio

tion shown previously to contain tumorigenic breast cancer cells (Al-Hajj et al. 2003). The tumorigenicity of low light scatter (resting) and high light scatter (differentiated) tumor populations were examined separately. For each of the four fractions, the total cells recovered after sorting were divided into four equal aliquots and injected into the mammary fat pad admixed with 10,000 heavily irradiated (10,000 rads) sorted $CD45^-$ tumor cells suspended in Matrigel. Thus animals received 43–58 sorted cells from the resting cell fractions and 633–13,200 cells from the more prevalent high scatter fractions (Fig. 4). Additionally, two groups of two mice each were injected at four sites each with 10,000 sorted $CD45^-$ unirradiated or irradiated tumor cells, respectively. All sorted $CD90^+$ cell fractions generated tumors, even the rare resting fractions where 43 and 58 cells were injected. The proportion of mice developing tumors and the day of sacrifice are shown in Fig. 4, with characteristic immunohistochemical staining for human cytokeratins. Tumors grew slowly and were first palpable at 5–10 months. Irradiated cells were not tumorigenic. None of the mice injected with sorted $CD45^-$cells evidenced tumors at the time that mice injected with $CD90^+$ cells were sacrificed. However, small tumors were observed in two of eight sites injected with $CD45^-$ cells when the experiment was terminated at day 371. Tumors were poorly differentiated with atypical nuclei.

Despite the homogeneity of the injected human cell populations, flow cytometry of tumor xenografts revealed a heterogeneity strikingly similar to the clinical isolate, regardless of the sorted population of origin. Figure 5 shows a detailed flow cytometric analysis of the freshly

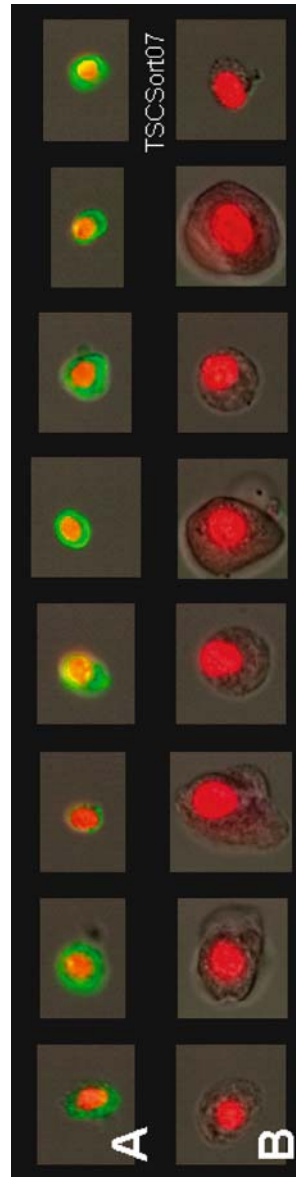
TSCSort07
A
B

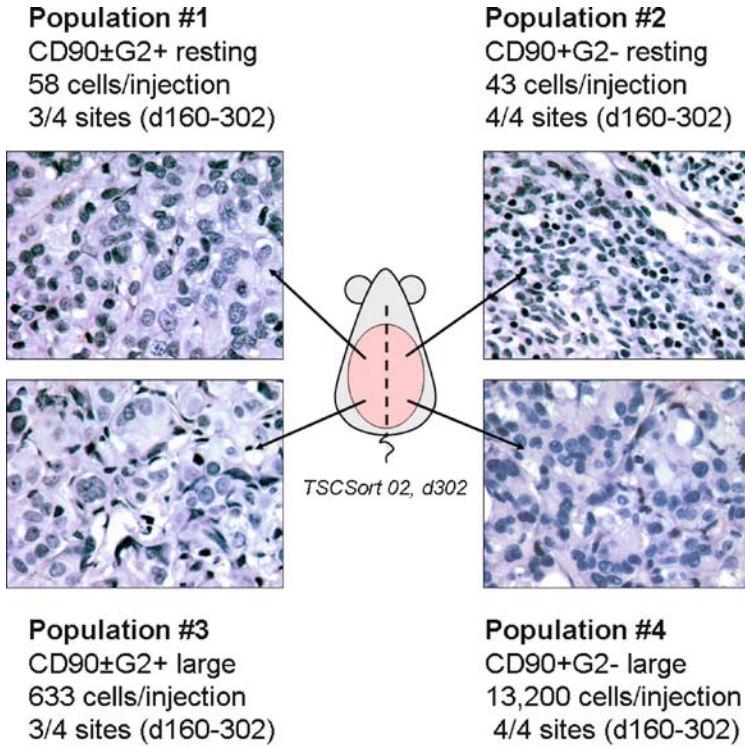

Fig. 4. In vivo tumorigenicity of ABCG2$^+$ and ABCG2$^-$ breast cancer cells. Twenty NOD/SCID mice were injected with FACS-sorted freshly isolated breast cancer pleural effusion cells as indicated. Sorted cells were admixed with 10,000 heavily irradiated CD45$^-$ tumor cells to minimize loss of small numbers of sorted tumor cells. The proportion of mice developing tumors and the days of sacrifice are indicated. Photomicrographs (×40 objective, H&E stain) illustrate histology on tumor xenografts harvested 302 days after injection of sorted cells. Tumors from all fractions were poorly differentiated, with abundant human cytokeratin$^+$ cells in most (not shown), but not all, tumors

isolated pleural effusion, sorted population 4 ($CD45^-$ $CD44^+$ $CD90^+$ $ABGG2^-$), and a tumor that was harvested 204 days after injection of this population. With the exception of human $CD45^+$ lymphohematopoietic cells, which were prevalent in the effusion and absent in the xenograft, all major effusion populations were observed in the xenograft. Interestingly, the injected population was present at a similar frequency in the original tumor and the effusion. This provides evidence for self-renewal and expansion of the $CD90^+$ $ABCG2^-$ fraction, since only 13,200 cells were injected and the resulting tumor measured 3 mm. Importantly, the injected $ABCG2^-$ cells gave rise to $ABCG2^+$ cells that were seen in both $CD90^+$ and $CD90^-$ fractions, as they were in the fresh clinical isolate.

To determine whether tumor xenografts could be passaged, tumors 1 and 4, harvested on day 302, were disaggregated and sorted into $CD45^-$ $CD44^+$ HEA^+ $CD90^+$ $ABCG2^-$ and $CD45^-$ $CD44^+$ HEA^+ $CD90^+$ $ABCG2^+$ fractions. Sorted cells were admixed with 10,000 irradiated unsorted tumor cells, suspended in Matrigel, and injected into the mammary fat pads of NOD/SCID mice (2 animals/fraction). The $CD90^+$ $ABCG2^-$ fraction from tumors 1 and 4 yielded 875 and 1,285 cells per injection site, respectively. The $CD90^+$ $ABCG2^+$ fraction from tumors 1 and 4 yielded 43,750 and 30,000 cells per injection site, respectively. Mice were sacrificed on days 129 and 231 with 3- to 8-mm subcutaneous tumors at the injection sites of all fractions.

3 Discussion

In this report we have demonstrated the existence of a rare population of $CD44^+$ $cytokeratin^+$ $ABCG2^+$ $CD90^+$ cells across a spectrum of previously untreated epithelial cancers, as well as in normal lung tissue. A proportion of these cells has resting morphology and coexpresses the stem/progenitor markers CD117 and CD133. The unexpected finding that the $ABCG2^+$ population and its subsets are detected at similar frequency in normal and neoplastic tissues, as well as across epithelial cancers from different organs, suggests that elements of normal epithelial stem cell function and differentiation are universally retained after neoplastic transformation. In contrast, great variability was seen in expres-

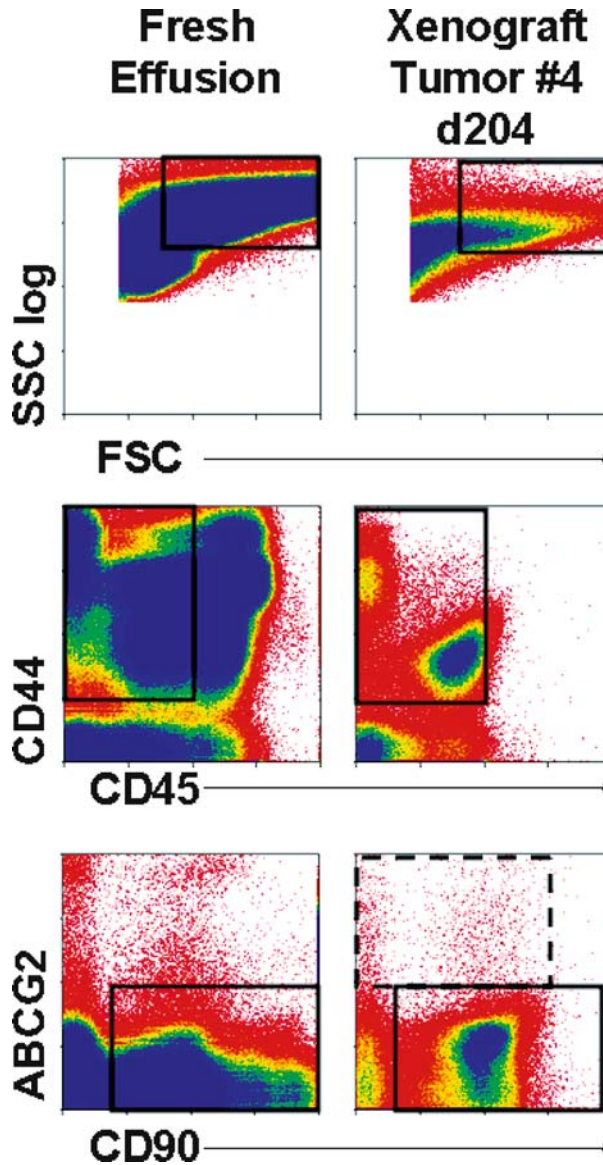
Fresh
Effusion
Xenograft
Tumor #4
d204
SSC log
FSC
CD44
CD45
ABCG2
CD90

Fig. 5. Self-renewal and differentiation in a breast cancer tumor stem cell xenograft. The *first column* shows seven-color flow cytometry performed on the freshly isolated breast cancer pleural effusion, which was sorted and injected into NOD/SCID mice. Superimposed are gates identical to those used to sort population 4 (high light scatter, $CD45^-$, $CD44^+$, $CD90^+$, $ABCG2^-$; 13,200 cells injected/mouse). The s*econd column* shows the tumor xenograft, which has differentiated substantially, showing light scatter heterogeneity, and the emergence of CD44 and CD90 negative populations. Most importantly, a population of $ABCG2^+$ cells (*dashed box*, 0.9%) was observed, indicating that MDR expression can be induced in the progeny of $ABCG2^-$ cells. Self-renewal can also be seen in the *solid boxes* (*column 2*), which indicate the xenograft tumor population falling within the original sort logic used to isolate population 4. Similar to the original pleural effusion, these cells comprised 13.1% of the xenograft tumor. However, since they arose from only 13,200 injected cells, the original $CD45^-$ $CD44^+$ $CD90^+$ $ABCG2^-$ cells expanded substantially within the xenograft tumor. Note: All histograms were gated on singlets (not shown). A total of 6 million effusion cells and 1.1 million xenograft tumor cells were analyzed

sion of maturation/differentiation markers (cytokeratin, MUC-1, HEA) between tumors from different organs, reflecting the different tissues of origin (data not shown). Interestingly, the frequency of $CD90^+$ and $CD117^+$ cells (candidate stem fraction) was lower and the frequency of $CD133^+$ cells (candidate progenitor fraction) was higher in untreated metastatic sites (Fig. 1).

Sorted $CD44^+$ $CD24^-$ breast cancer cells (Al-Hajj et al. 2003), as well as sorted $CD133^+$ cells from brain tumors (Singh et al. 2004) and prostate cancer (Collins et al. 2005), have previously been shown to be tumorigenic in NOD/SCID mice. Although these studies have been widely quoted as supporting the cancer stem cell hypothesis, they did not attempt to distinguish between stem and progenitor compartments and did not determine whether the tumorigenic fraction was protected by mechanisms common to normal tissue stem cells. In this report we used the markers CD90, CD117 and CD133 to identify the stem/progenitor fraction within the $CD45^-$ $CD44^+$ compartment. Within this population, low morphologic complexity and the differentiation

marker HEA were used to provisionally distinguish between resting stem cells and more differentiated progenitor cells. We found that both stem and progenitor populations are tumorigenic, and both have a subset that expresses the ABC transporter ABCG2. However, only the resting stem cell fraction had a subpopulation with constitutive activity of both ABCG2 and ABCB1 transporters (Fig. 2). Further, the stem cell fraction was tumorigenic at very high frequency.

Biologically, the salient finding is that untreated epithelial tumors retain a vestige of the ordered growth and differentiation of the parent tissue, including the persistence of resting stemlike cells (some of which are protected by MDR transporters), a more differentiated tumorigenic progenitor fraction, and their postmitotic nonclonogenic progeny. Despite the phenotypic heterogeneity of tumorigenic cells, the most critical population from a therapeutic standpoint is the resting stem cell-like population. We hypothesize that this population is as resistant to cytotoxic therapy as its normal counterpart, by virtue of constitutive MDR activity and possibly other protective mechanisms afforded by the niche in which it persists (Arai et al. 2005). This population provides an attractive candidate for the cancer stem cell postulated by Weissman (Reya et al. 2001; Al-Hajj et al. 2004) Dick (Dick 2003; Dick and Lapidot 2005) and others: a resting, drug resistant tumor cell that can lay dormant after initially successful therapy, providing a seed for later recurrence and metastasis.

The finding of intrinsic MDR activity within a rare resting tumorigenic population is not explained by the conventional MDR paradigm, which views ABC transporter-mediated drug resistance as a trait that tumor cells acquire on drug exposure through substrate-driven induction, gene amplification, or regional gene activation. By concentrating on freshly isolated therapy-naive clinical isolates, we have demonstrated that ABC transporter expression and activity is present before exposure to cytotoxic agents. Given the central role of MDR transporters in protecting normal tissue stem cells, our data support a broadened interpretation of the cancer stem cell paradigm, and provide a unified explanation for the successes and failures of cytotoxic antineoplastic therapy. Namely, the ultimate target, the MDR-protected resting cancer stem cell, is spared along with its normal tissue stem cell counterparts. Since cytotoxic regimens must be designed to minimize irre-

versible toxicity to normal tissue, the therapeutic index has traditionally been thought of as the differential sensitivity of measurable tumor versus that of the highly protected adult tissue stem cell compartment, which is required for regeneration. Our findings recast this concept as the differential sensitivity of MDR-protected tumor stem cells and their normal tissue counterparts.

4 Methods

4.1 Patient Samples

Thirty-four patient samples (tumor, adjacent normal tissue, ascites, and pleural effusions) were acquired under protocols approved by the University of Pittsburgh Internal Review Board. With the exception of the sample described in Figs. 4 and 5, all were obtained from patients at the time of tumor resection and before cytotoxic or radiation therapy.

4.2 Tissue Digestion

Solid tissues were minced with paired scalpels, digested with type I collagenase (4% in RPMI 1640 medium, Sigma Chemicals, St. Louis, MO) (Elder and Whiteside 1992) and disaggregated through 100 mesh stainless steel screens. Ten to 500 million viable cells were recovered from 5 to 10 mm^3 specimens of tumor or normal lung parenchyma. Pleural effusions and ascites were concentrated, collagenase digested, and separated on a ficoll/hypaque gradient.

4.3 Staining and Flow Cytometry

Single cell suspensions were stained according to a protocol described in detail elsewhere (Donnenberg and Donnenberg 2003). Five minutes before staining with fluorochrome-conjugated monoclonal antibodies, neat mouse serum (5 μL) was added to each cell pellet to minimize nonspecific antibody binding. Before cytokeratin staining, cells were stained for surface markers and permeabilized with 0.1% saponin (Beckman Coulter, Fullerton, CA) in phosphate-buffered saline with 0.5% human serum albumin. Antibodies and dyes used in these studies included HEA-FITC (Miltenyi Biotech, Bergisch Gladbach, Ger-

many, Cat. No. 12000420), pan cytokeratin-FITC (Beckman Coulter, Cat.
No. IM2356), CD44-PE (Serotec, Oxford, UK, Cat. No. MCA 89PE); CD90-biotin (BD, Cat. No. 555594), streptavidin-ECD (Beckman Coulter, Cat. No. IM3326), ABCG2-PC5 (Chemicon, Temecula, CA, Cat. No. MAB4155PC), CD117-PC7 (Beckman Coulter, Cat. No. IM3698), CD133-APC (Miltenyi Biotech, Cat. No. 120001241), CD45-APCC7 (BD, Cat. No. 557833), propidium iodide (Calbiochem, La Jolla, CA, Cat. No. 537059), rhodamine 123 (Sigma Chemicals, St. Louis MO, Cat. No. R8004), Hoechst 33342 (Invitrogen, Carlsbad, CA, Cat. No. H3570), and Draq5 (Alexis Biochemicals, Lausen, Switzerland, Cat. No. BOS-889-001-R200). Fumitremorgin was purchased from Alexis (Cat. No. ALX-350-127). Seven-color analysis was performed with the three-laser, nine-color CyAn LX cytometer (DakoCytomation, Fort Collins, CO). Sorting and analysis requiring an ultraviolet laser was performed on a three-laser, eight-color DakoCytomation MoFlo. An effort was made to acquire a total of 5 million cells per sample at rates not exceeding 10,000 events/s. The cytometers were calibrated before each use with SpectrAlign beads (DakoCytomation, Cat. No. KO111) and eight-peak Rainbow Calibration Particles (Spherotech, Libertyville, IL, Cat. No. RCP-30-5A). Color compensation matrixes were calculated for each staining combination within each experiment, using single-stained mouse IgG capture beads (Becton Dickinson, Cat. No. 552843) for each antibody and single-stained cells for rhodamine 123. Off-line analysis was performed with Summit software (DakoCytomation). In all analyses, doublets and clusters were eliminated with forward scatter peak width versus height as a discriminator. Propidium iodide staining was used to eliminate nonviable cells.

4.4 Tumor Xenografts

Female NOD.CB17-Prkdcscid/J mice 6–8 weeks of age were purchased from The Jackson Laboratory (Bar Harbor, ME), and housed five to a cage in a specific pathogen-free environment. Before injection of tumor cells, mice were anesthetized by methoxyflurane inhalation. Sorted cells were admixed with sorted $CD45^-$ tumor (irradiated with 10,000 rads from a ^{137}Cs source) and suspended in 25 μL of ice-cold DMEM, 15%

FBS, plus 25 μL of Matrigel (Becton Dickinson). Fifty microliters of ice-cold cell suspension were injected subcutaneously into the mammary fatpads (4 injections/animal). Animals were examined twice weekly for behavioral changes and evidence of tumor.

4.5 Statistical Analysis

The frequencies of cells expressing stem cell markers were compared with Student's *t*-test for two groups (2-tailed test). Statistical tests, descriptive statistics, and graphic analysis (other than cytometry) were performed with Systat version 11 (Systat Software Inc, Richmond, CA).

Acknowledgements. Supported by Grants BC032981 and BC044784 from the Department of Defense, the Hillman Foundation, and The Glimmer of Hope Foundation. Vera S. Donnenberg is the recipient of a Department of Defense Era of Hope Scholar Award.

References

Al-Hajj M, Wicha MS, Benito-Hernandez A, Morrison SJ, Clarke MF (2003) Prospective identification of tumorigenic breast cancer cells. Proc Natl Acad Sci USA 100:3983–3988

Al-Hajj M, Becker MW, Wicha M, Weissman I, Clarke MF (2004) Therapeutic implications of cancer stem cells. Curr Opin Genet Dev 14:43–47

Alonso L, Fuchs E (2003) Stem cells of the skin epithelium. Proc Natl Acad Sci USA 100(1):11830–11835

Arai F, Hirao A, Suda T (2005) Regulation of hematopoietic stem cells by the niche. Trends Cardiovasc Med 15:75–79

Bertoncello I, Williams B (2004) Hematopoietic stem cell characterization by Hoechst 33342 and rhodamine 123 staining. In: Hawley TS, Hawley RG (eds) Methods in molecular biology: flow cytometry protocols, 2nd edn. Humana Press, Totowa, NJ

Biedler JL, Riehm H (1970) Cellular resistance to actinomycin D in Chinese hamster cells in vitro: cross-resistance, radioautographic, and cytogenetic studies. Cancer Res 30:1174–1184

Chaudhary PM, Roninson IB (1991) Expression and activity of P-glycoprotein, a multidrug efflux pump, in human hematopoietic stem cells. Cell 66:85–94

Chen GK, Lacayo NJ, Duran GE, Wang Y, Bangs CD, Rea S, Kovacs M, Cherry AM, Brown JM, Sikic BI (2002) Preferential expression of a mutant allele of the amplified MDR1 (ABCB1) gene in drug-resistant variants of a human sarcoma. Genes Chromosomes Cancer 34:372–383

Chen J, Hersmus N, Van Duppen V, Caesens P, Denef C, Vankelecom H (2005) The adult pituitary contains a cell population displaying stem/progenitor cell and early embryonic characteristics. Endocrinology 146:3985–3998

Collins AT, Berry PA, Hyde C, Stower MJ, Maitland NJ (2005) Prospective identification of tumorigenic prostate cancer stem cells. Cancer Res 65:10946–10951

Dick JE (2003) Breast cancer stem cells revealed. Proc Natl Acad Sci USA 100:3547–3549

Dick JE, Lapidot T (2005) Biology of normal and acute myeloid leukemia stem cells. Int J Hematol 82:389–396

Donnenberg VS, Donnenberg AD (2003) Identification, rare-event detection and analysis of dendritic cell subsets in broncho-alveolar lavage fluid and peripheral blood by flow cytometry. Front Biosci 8:1175–1180

Donnenberg VS, Donnenberg AD (2005) Multiple drug resistance in cancer revisited: the cancer stem cell hypothesis. J Clin Pharmacol 45:872–877

Elder EM, Whiteside TL (1992) Processing of tumors for vaccine and/or tumor infiltrating lymphocytes. In: Rose NR, Conway de Macario E, Fahey JL, Friedman H, Penn GM (eds) Manual of clinical laboratory immunology, 4th edn. American Society for Microbiology, Washington, DC, pp 817–819

Fiala S (1968) The cancer cell as a stem cell unable to differentiate. A theory of carcinogenesis. Neoplasma 15:607–622

Giangreco A, Shen H, Reynolds SD, Stripp BR (2004) Molecular phenotype of airway side population cells. Am J Physiol Lung Cell Mol Physiol 286:L624–L630

Goodell MA, Brose K, Paradis G, Conner AS, Mulligan RC (1996) Isolation and functional properties of murine hematopoietic stem cells that are replicating in vivo. J Exp Med 183:1797–1806

Hamburger AW, Salmon SE (1977) Primary bioassay of human tumor stem cells. Science 197:461–463

He DN, Qin H, Liao L, Li N, Zhu WM, Yu BJ, Wu X, Zhao RC, Li JS (2005) Small intestinal organoid-derived SP cells contribute to repair of irradiation-induced skin injury. Stem Cells Dev 14:285–291

Leslie EM, Deeley RG, Cole SP (2005) Multidrug resistance proteins: role of P-glycoprotein, MRP1, MRP2, and BCRP (ABCG2) in tissue defense. Toxicol Appl Pharmacol 204:216–237

Ling V, Thompson LH (1974) Reduced permeability in CHO cells as a mechanism of resistance to colchicine. J Cell Physiol 83:103–116

Paus R, Cotsarelis G (1999) The biology of hair follicles. N Engl J Med 341:491–497

Polyak K, Hahn WC (2006) Roots and stems: stem cells in cancer. Nat Med 12:296–300

Rendl M, Lewis L, Fuchs E (2005) Molecular dissection of mesenchymal-epithelial interactions in the hair follicle. PLoS Biol 3:e331

Reya T, Morrison SJ, Clarke MF, Weissman IL (2001) Stem cells, cancer, and cancer stem cells. Nature 414:105–111

Riou L, Bastos H, Lassalle B, Coureuil M, Testart J, Boussin FD, Allemand I, Fouchet P (2005) The telomerase activity of adult mouse testis resides in the spermatogonial alpha6-integrin-positive side population enriched in germinal stem cells. Endocrinology 146:3926–3932

Singh SK, Hawkins C, Clarke ID, Squire JA, Bayani J, Hide T, Henkelman RM, Cusimano MD, Dirks PB (2004) Identification of human brain tumour initiating cells. Nature 432:396–401

Udomsakdi C, Eaves CJ, Sutherland HJ, Lansdorp PM (1991) Separation of functionally distinct subpopulations of primitive human hematopoietic cells using rhodamine-123. Exp Hematol 19:338–342

Wang YC, Juric D, Francisco B, Yu RX, Duran GE, Chen GK, Sikic BI (2006) Regional activation of chromosomal arm 7q with and without gene amplification in taxane-selected human ovarian cancer cell lines. Genes Chromosomes Cancer 45:365–374

Watt FM (1998) Epidermal stem cells: markers, patterning and the control of stem cell fate. Philos Trans R Soc Lond B Biol Sci 353:831–837

Webb M, Raphael CL, Asbahr H, Erber WN, Meyer BF (1996) The detection of rhodamine 123 efflux at low levels of drug resistance. Br J Haematol 93:650–655

Wicha MS, Liu S, Dontu G (2006) Cancer stem cells: an old idea—a paradigm shift. Cancer Res 66:1883–1890

Yano S, Ito Y, Fujimoto M, Hamazaki TS, Tamaki K, Okochi H (2005) Characterization and localization of side population cells in mouse skin. Stem Cells 23:834–841